

# Steric and Electronic Control of the Spin State in Three-Fold Symmetric, Four-Coordinate Iron(II) Complexes

Hsiu-Jung Lin,<sup>†,‡</sup> Diana Siretanu,<sup>§,||</sup> Diane A. Dickie,<sup>⊥</sup> Deepak Subedi,<sup>†</sup> Jeremiah J. Scepaniak,<sup>†</sup> Dmitri Mitcov,<sup>§,||</sup> Rodolphe Clérac,<sup>\*,§,||</sup> and Jeremy M. Smith<sup>\*,†,‡</sup>

<sup>†</sup>Department of Chemistry and Biochemistry, New Mexico State University, Las Cruces, New Mexico 88003, United States

<sup>‡</sup>Department of Chemistry, Indiana University, 800 East Kirkwood Avenue, Bloomington, Indiana 47405, United States

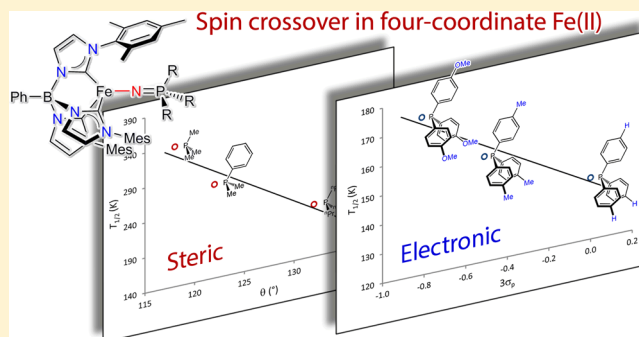
<sup>§</sup>CNRS, CRPP, UPR 8641, F-33600 Pessac, France

<sup>||</sup>Univ. Bordeaux, CRPP, UPR 8641, F-33600 Pessac, France

<sup>⊥</sup>Department of Chemistry, The University of New Mexico, Albuquerque, New Mexico 87131, United States

## Supporting Information

**ABSTRACT:** The three-fold symmetric, four-coordinate iron(II) phosphoraminate complexes  $\text{PhB}(\text{MesIm})_3\text{Fe}-\text{N}=\text{PRR}'\text{R}''$  ( $\text{PRR}'\text{R}'' = \text{PMePh}_2, \text{PMe}_2\text{Ph}, \text{PMe}_3,$  and  $\text{P}^n\text{Pr}_3$ ) undergo a thermally induced  $S = 0$  to  $S = 2$  spin-crossover in fluid solution. Smaller phosphoraminate ligands stabilize the low-spin state, and an excellent correlation is observed between the characteristic temperature of the spin-crossover ( $T_{1/2}$ ) and the Tolman cone angle ( $\theta$ ). Complexes with *para*-substituted triaryl phosphoraminate ligands ( $p\text{-XC}_6\text{H}_4$ )<sub>3</sub>P=N<sup>-</sup> ( $X = \text{H}, \text{Me}$  and  $\text{OMe}$ ) also undergo spin-crossover in solution. These isosteric phosphoraminate ligands reveal that the low-spin state is stabilized by more strongly donating ligands. This control over the spin state provides important insights for modulating the magnetic properties of four-coordinate iron(II) complexes.



## INTRODUCTION

Transition metal complexes with  $d^4$ – $d^7$  electron configurations may exhibit more than one accessible spin state. For a narrow range of ligand field strengths, at least two spin states may be thermally accessible, leading to a thermal equilibrium. This so-called spin-crossover phenomenon is characterized by the temperature,  $T_{1/2}$ , for which the population of each state is equal.<sup>1</sup> Six-coordinate iron(II) complexes are by far the most prevalent class of spin-crossover compounds,<sup>2</sup> with most complexes based on an  $\text{FeN}_6$  coordination sphere, although other donor sets are known.<sup>1,2</sup>

Given the small energy differences associated with spin-crossover, it is not surprising that the phenomenon is sensitive to small environmental changes, including changes to the ligand environment. For example, the iron(II) complex  $[\text{Fe}(\text{py})_4(\text{NCS})_2]$  is high spin at all temperatures, but substituting in a stronger field phenanthroline ligand induces spin-crossover in the solid state ( $[\text{Fe}(\text{phen})(\text{py})_2(\text{NCS})_2]$ ,  $T_{1/2} = 106$  K).<sup>3</sup> Substituting in an additional phenanthroline ligand further increases the solid-state spin-crossover temperature ( $[\text{Fe}(\text{phen})_2(\text{NCS})_2]$ ,  $T_{1/2} = 176$  K).<sup>4</sup> More subtly, phenanthroline ligand modifications can also impact spin-crossover behavior. Thus, increasing the field strength of the phenanthroline ligand by ligand alkylation stabilizes the low-spin state ( $[\text{Fe}(4\text{-Mephen})_2(\text{NCS})_2]$ ,  $T_{1/2} = 215$  K).<sup>5</sup> On the

other hand,  $[\text{Fe}(2\text{-Mephen})_2(\text{NCS})_2]$  has a high-spin ground state,<sup>6</sup> which is likely a consequence of steric interactions involving the 2-methyl substituent that lengthens the metal–ligand bond and consequently reduces the ligand field strength.

We recently reported that the iron(II) phosphoraminate complex  $\text{PhB}(\text{MesIm})_3\text{Fe}-\text{N}=\text{PPh}_3$  undergoes a thermally induced  $S = 0$  to  $S = 2$  spin-crossover (Figure 1),<sup>7</sup> observed by SQUID magnetometry and Mössbauer spectroscopy at  $T_{1/2} = 81$  K in the solid state. Temperature-dependent X-ray crystallography reveals that the  $S = 0$  to  $S = 2$  crossover is accompanied, as expected, by an increase in the both the Fe–C and Fe–N bond lengths.

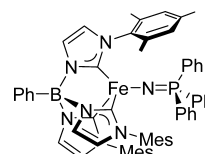
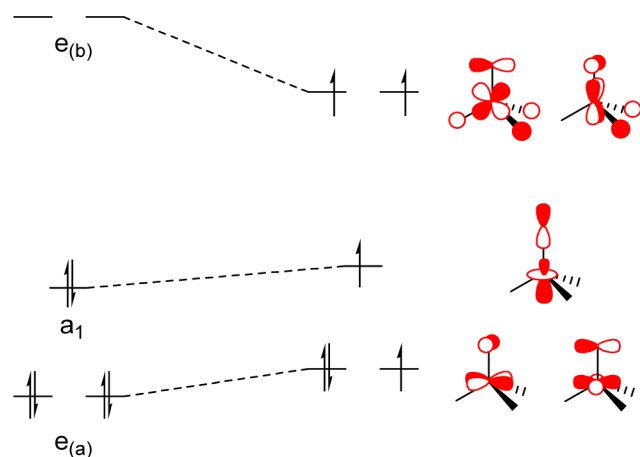


Figure 1. Schematic structure of  $\text{PhB}(\text{MesIm})_3\text{Fe}-\text{N}=\text{PPh}_3$ .

Received: July 1, 2014

Published: August 26, 2014

The structural and spectroscopic changes associated with the spin-crossover have been interpreted in terms of a simple molecular orbital picture (Figure 2). This model predicts that



**Figure 2.** Electronic structure diagram illustrating the spin-crossover in  $\text{PhB}(\text{MesIm})_3\text{Fe-N}=\text{PPh}_3$ .

the extent of  $\pi$ -bonding between iron and phosphoraminate ligand,  $\text{R}_3\text{P}=\text{N}^-$ , is likely to play a key role in modulating the spin-crossover temperature, specifically by either stabilizing or destabilizing the  $e_{(b)}$  orbital set.<sup>8</sup> Changes to this single ligand may be expected to modify the spin-state energy scheme of the complex.

Both the size and the donor strength of the phosphoraminate ligand are expected to affect the extent of Fe–N  $\pi$ -bonding. Smaller phosphoraminate ligands will destabilize the  $e_{(b)}$  orbital set by virtue of their shorter Fe–N bonds, whereas more basic ligands will destabilize these orbitals as a result of their greater donor strength. Thus, smaller, more basic phosphoraminate ligands are expected to stabilize the low-spin state.

In contrast to six-coordinate complexes, few low-coordinate iron complexes have been reported to exhibit the spin-crossover phenomenon.<sup>9–11</sup> Because low-coordinate environments are often used to stabilize metal–ligand multiple bonds for complexes having high d-electron counts,<sup>12–15</sup> delineating the factors that control the spin state in this environment is important for understanding the reactivity of these species. Additionally, certain four-coordinate spin-crossover complexes may have advantageous properties for information storage applications<sup>16</sup> resulting from their photoinduced single molecule magnet behavior.<sup>17</sup>

This article reports an investigation into the steric and electronic effects of the phosphoraminate ligand on the spin-crossover behavior of four-coordinate iron(II) tris(carbene)borate complexes.<sup>18</sup> The spin-crossover behavior of two sets of complexes has been investigated in fluid solution by VT NMR and fluid/frozen solutions by SQUID magnetometry, eliminating the impact of solid-state packing effects. The phosphoraminate ligands in these complexes vary in their steric and electronic properties, allowing for quantitative relationships between the spin-crossover temperature and ligand properties to be established.

## EXPERIMENTAL SECTION

**General Considerations.** Manipulations involving air-sensitive materials were performed under a nitrogen atmosphere by standard

Schlenk techniques or in an MBraun Labmaster glovebox. The quality of the glovebox atmosphere was periodically checked with a toluene solution of titanocene.<sup>19</sup> Glassware was dried at 150 °C overnight. Diethyl ether, pentane, tetrahydrofuran, and toluene were purified by the Glass Contour solvent purification system. Deuterated benzene was dried first over  $\text{CaH}_2$  and then over Na/benzophenone before vacuum transfer into a storage container, whereas THF- $d_8$  was dried over molecular sieves. Before use, aliquots of  $\text{Et}_2\text{O}$ , THF, and toluene were tested with a drop of Na/benzophenone in THF solution. The iron(IV) nitride starting material  $\text{PhB}(\text{MesIm})_3\text{Fe}\equiv\text{N}^{13j}$  was prepared according a literature procedure and recrystallized three times by slow diffusion of pentane into a saturated THF solution at  $-35$  °C. The triarylphosphine complexes  $\text{PhB}(\text{MesIm})_3\text{Fe-N}=\text{P}(p\text{-XC}_6\text{H}_4)_3$  (X = H 5,  $\text{CF}_3$  6, Me 7 and OMe 8) have been previously reported.<sup>13o</sup> The complexes were recrystallized by slow diffusion of pentane into a saturated THF solution at  $-35$  °C. All other chemicals were obtained commercially and used as received.  $^1\text{H}$  NMR data were recorded on a Varian Unity 400 spectrometer (400 MHz) at 22 °C. All resonances in the  $^1\text{H}$  NMR spectra are referenced to residual  $\text{C}_6\text{D}_5\text{H}$  ( $\delta$  7.16 ppm) or  $\text{C}_4\text{D}_7\text{HO}$  ( $\delta$  3.57 and 1.72 ppm). UV–vis spectra were recorded on an Agilent Technologies Cary 60 UV–vis, whereas IR spectra were recorded on a PerkinElmer Spectrum Two FTIR spectrometer. Elemental analyses were performed by Robertson MicroLab Laboratories (Madison, NJ) and Midwest MicroLab (Indianapolis, IN).

**Synthesis of Complexes.** A solution of  $\text{PhB}(\text{MesIm})_3\text{Fe}\equiv\text{N}$  (ca. 50 mg) and the corresponding phosphine (1 equiv) was stirred in THF (5 mL) at room temperature for 1 h. The solvent was removed *in vacuo*, and the product was crystallized as described below.

**$\text{PhB}(\text{MesIm})_3\text{Fe-N}=\text{PMePh}_2$  (1).** A green solution of 1 formed immediately. Green crystals were obtained from slow diffusion of pentane into a saturated THF solution at  $-35$  °C (72% yield).  $^1\text{H}$  NMR ( $\text{C}_6\text{D}_6$ ) 25 °C:  $\delta$  78.7 (3H, Im-H), 65.6 (3H, Im-H), 58.5 (3H, P(MePh)<sub>2</sub>), 53.0 (4H, P(MePh)<sub>2</sub> o/m-H), 51.0 (2H, B(C<sub>6</sub>H<sub>5</sub>)<sub>3</sub> o/m-H), 24.8 (2H, B(C<sub>6</sub>H<sub>5</sub>)<sub>3</sub> o/m-H), 22.8 (4H, P(MePh)<sub>2</sub> o/m-H), 21.2 (1H, B(C<sub>6</sub>H<sub>5</sub>)<sub>3</sub> p-H), 11.8 (2H, P(MePh)<sub>2</sub> p-H), 2.6 (9H, Mes p-Me),  $-2.6$  (6H, Mes m-H),  $-46.3$  (18H, Mes o-Me).  $^1\text{H}$  NMR (THF- $d_8$ ) 25 °C:  $\delta$  78.6 (3H, Im-H), 65.1 (3H, Im-H), 54.8 (3H, P(MePh)<sub>2</sub>), 52.2 (4H, P(MePh)<sub>2</sub> o/m-H), 49.6 (2H, B(C<sub>6</sub>H<sub>5</sub>)<sub>3</sub> o/m-H), 24.3 (2H, B(C<sub>6</sub>H<sub>5</sub>)<sub>3</sub> o/m-H), 22.7 (4H, P(MePh)<sub>2</sub> o/m-H), 20.9 (1H, B(C<sub>6</sub>H<sub>5</sub>)<sub>3</sub> p-H), 11.9 (2H, P(MePh)<sub>2</sub> p-H), 2.6 (9H, Mes p-Me),  $-2.4$  (6H, Mes m-H),  $-44.8$  (18H, Mes o-Me).  $\mu_{\text{eff}} = 4.7(3)\mu_{\text{B}}$  (298 K). Anal. Calcd for  $\text{C}_{55}\text{H}_{57}\text{BFeN}_7\text{P}$ : C, 72.30; H, 6.29; N, 10.73. Found: C, 72.27; H, 6.27; N, 10.68.

**$\text{PhB}(\text{MesIm})_3\text{Fe-N}=\text{PMe}_2\text{Ph}$  (2).** A purple solution of 2 formed immediately. Dark blue crystals were obtained by slow diffusion of pentane into a saturated  $\text{Et}_2\text{O}$  solution at  $-35$  °C (82% yield).  $^1\text{H}$  NMR ( $\text{C}_6\text{D}_6$ ) 25 °C:  $\delta$  61.6 (3H, Im-H), 51.5 (3H, Im-H), 47.6 (6H, P(Me<sub>2</sub>Ph)), 43.5 (2H, P(Me<sub>2</sub>Ph) o/m-H), 40.3 (2H, B(C<sub>6</sub>H<sub>5</sub>)<sub>3</sub> o/m-H), 20.4 (2H, B(C<sub>6</sub>H<sub>5</sub>)<sub>3</sub> o/m-H), 18.9 (2H, P(Me<sub>2</sub>Ph) o/m-H), 17.8 (1H, B(C<sub>6</sub>H<sub>5</sub>)<sub>3</sub> p-H), 12.0 (1H, P(Me<sub>2</sub>Ph) p-H), 2.4 (9H, Mes p-Me),  $-0.3$  (6H, Mes m-H),  $-33.2$  (18H, Mes o-Me).  $^1\text{H}$  NMR (THF- $d_8$ ) 25 °C:  $\delta$  58.4 (3H, Im-H), 49.6 (3H, Im-H), 45.3 (6H, P(Me<sub>2</sub>Ph)), 41.1 (2H, P(Me<sub>2</sub>Ph) o/m-H), 38.3 (2H, B(C<sub>6</sub>H<sub>5</sub>)<sub>3</sub> o/m-H), 19.8 (2H, B(C<sub>6</sub>H<sub>5</sub>)<sub>3</sub> o/m-H), 18.3 (2H, P(Me<sub>2</sub>Ph) o/m-H), 17.2 (1H, B(C<sub>6</sub>H<sub>5</sub>)<sub>3</sub> p-H), 11.7 (1H, P(Me<sub>2</sub>Ph) p-H), 2.4 (9H, Mes p-Me), 0.1 (6H, Mes m-H),  $-31.3$  (18H, Mes o-Me).  $\mu_{\text{eff}} = 4.0(3)\mu_{\text{B}}$  (298 K). Repeated elemental analysis measurements were consistently low in carbon content.

**$\text{PhB}(\text{MesIm})_3\text{Fe-N}=\text{PMe}_3$  (3).** A purple solution of 3 formed immediately. Purple crystals were obtained by slowly diffusing pentane from a saturated solution into Paratone oil at  $-35$  °C (56% yield).  $^1\text{H}$  NMR ( $\text{C}_6\text{D}_6$ ) 25 °C:  $\delta$  20.5 (3H, Im-H), 17.5 (3H, Im-H), 15.9 (2H, B(C<sub>6</sub>H<sub>5</sub>)<sub>3</sub> o/m-H), 12.8 (9H, PMe<sub>3</sub>), 10.6 (2H, B(C<sub>6</sub>H<sub>5</sub>)<sub>3</sub> o/m-H), 9.9 (1H, B(C<sub>6</sub>H<sub>5</sub>)<sub>3</sub> p-H), 5.0 (6H, Mes m-H), 2.2 (9H, Mes p-Me),  $-6.2$  (18H, Mes o-Me).  $^1\text{H}$  NMR (THF- $d_8$ ) 25 °C:  $\delta$  19.2 (3H, Im-H), 17.0 (3H, Im-H), 15.0 (2H, B(C<sub>6</sub>H<sub>5</sub>)<sub>3</sub> o/m-H), 11.9 (9H, PMe<sub>3</sub>), 10.3 (2H, B(C<sub>6</sub>H<sub>5</sub>)<sub>3</sub> o/m-H), 9.6 (1H, B(C<sub>6</sub>H<sub>5</sub>)<sub>3</sub> p-H), 5.2 (6H, Mes m-H), 2.3 (9H, Mes p-Me),  $-5.6$

Scheme 1

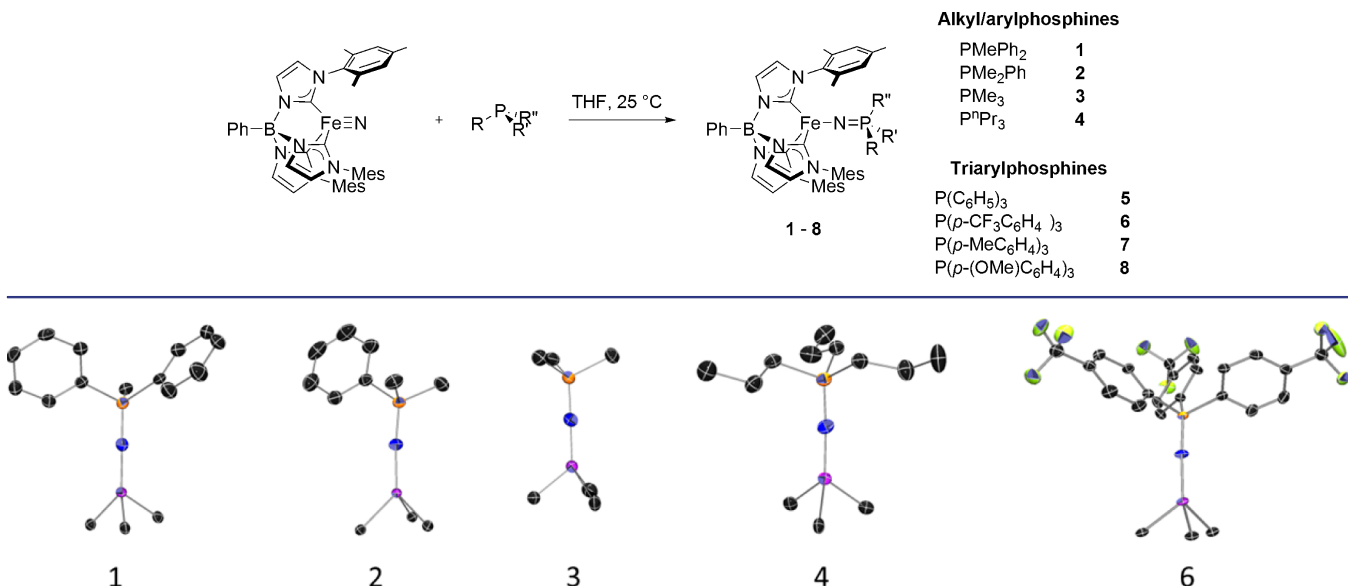


**Figure 3.** Solid-state structures of complexes 1–4 and 6. Thermal ellipsoids are shown at 50% probability; hydrogen atoms and most of the tris(carbene)borate ligand are omitted for clarity. Black, blue, orange, purple, and green ellipsoids represent C, N, P, Fe, and F atoms, respectively.

(18H, Mes *o*-Me).  $\mu_{\text{eff}} = 1.7(3)\mu_{\text{B}}$  (298 K). Due to the extreme air-sensitivity of this complex, we have been unable to obtain satisfactory elemental analysis data.

**PhB(MesIm)<sub>3</sub>Fe–N=P<sup>n</sup>Pr<sub>3</sub> (4).** A yellow–green solution of 4 formed immediately. Yellow–green crystals were obtained by slow diffusion of pentane into a saturated THF solution at –35 °C (43% yield). <sup>1</sup>H NMR (C<sub>6</sub>D<sub>6</sub>) 25 °C:  $\delta$  73.6 (3H, Im-H), 73.6 (6H, P(CH<sub>2</sub>CH<sub>2</sub>CH<sub>3</sub>)<sub>3</sub>), 60.5 (3H, Im-H), 47.7 (2H, B(C<sub>6</sub>H<sub>5</sub>)<sub>3</sub> *o/m*-H), 32.8 (6H, P(CH<sub>2</sub>CH<sub>2</sub>CH<sub>3</sub>)<sub>3</sub>), 23.4 (2H, B(C<sub>6</sub>H<sub>5</sub>)<sub>3</sub> *o/m*-H), 20.2 (1H, B(C<sub>6</sub>H<sub>5</sub>)<sub>3</sub> *p*-H), 12.2 (9H, P(CH<sub>2</sub>CH<sub>2</sub>CH<sub>3</sub>)<sub>3</sub>), 1.5 (9H, Mes *p*-Me), –2.8 (6H, Mes *m*-H), –40.7 (18H, Mes *o*-Me). <sup>1</sup>H NMR (THF-*d*<sub>8</sub>) 25 °C:  $\delta$  73.1 (3H, Im-H), 73.1 (6H, P(CH<sub>2</sub>CH<sub>2</sub>CH<sub>3</sub>)<sub>3</sub>), 60.5 (3H, Im-H), 47.4 (2H, B(C<sub>6</sub>H<sub>5</sub>)<sub>3</sub> *o/m*-H), 32.8 (6H, P(CH<sub>2</sub>CH<sub>2</sub>CH<sub>3</sub>)<sub>3</sub>), 23.5 (2H, B(C<sub>6</sub>H<sub>5</sub>)<sub>3</sub> *o/m*-H), 20.2 (1H, B(C<sub>6</sub>H<sub>5</sub>)<sub>3</sub> *p*-H), 11.9 (9H, P(CH<sub>2</sub>CH<sub>2</sub>CH<sub>3</sub>)<sub>3</sub>), 1.5 (9H, Mes *p*-Me), –2.7 (6H, Mes *m*-H), –40.6 (18H, Mes *o*-Me).  $\mu_{\text{eff}} = 5.7(3)\mu_{\text{B}}$  (298 K). Anal. Calcd for C<sub>51</sub>H<sub>65</sub>BF<sub>6</sub>FeN<sub>7</sub>P: C, 70.11; H, 7.50; N, 11.22. Found: C, 69.86; H, 7.33; N, 11.16.

**Solution Magnetic Studies.** Solution magnetic studies for 1–4 were conducted by variable temperature <sup>1</sup>H NMR spectroscopy. A resealable NMR tube was charged with phosphoraminate complex (ca. 6 mg), THF-*d*<sub>8</sub> (400 mg), and a sealed capillary of THF-*d*<sub>8</sub>. <sup>1</sup>H NMR spectra were recorded between 200 and 328 K. The temperature was calibrated using 100% ethylene glycol (300–380 K) and 100% methanol (180–300 K). The magnetic susceptibility measurements for complexes 5–8 were obtained with the use of a Quantum Design SQUID magnetometer MPMS-XL. This magnetometer works between 1.8 and 400 K for dc applied fields ranging from –7 to 7 T. Measurements in solution of 3 mmol/L concentration were carried out in sealed plastic straws under argon. It is worth noting that the chosen concentrations for the magnetic measurements were determined after multiple tests down to 77 K to avoid precipitation of powder and/or crystals during cooling. The field-dependent magnetization was systematically measured at 100 K on each sample in order to detect the presence of any ferromagnetic impurities. Paramagnetic or diamagnetic materials should exhibit a perfectly linear dependence of the magnetization that extrapolates to zero at zero dc field. The samples appeared to be free of any significant ferromagnetic impurities and moreover the susceptibility obtained from the slope of the *M* versus *H* plots at 100 K was always in good agreement with the

susceptibility measurements at 0.1 or 1 T. Magnetic data were then corrected for the sample holder, the residual low temperature paramagnetism (due to the partial decomposition of these extremely air-sensitive samples), and diamagnetic contributions for all magnetic measurements. Therefore, after these corrections, the magnetic data shown in Figures 7, S11, and S12 are presented normalized between 0 and 1 to discuss the thermal spin-crossover of the studied compounds. Data before normalization are also shown (Figures S10–S12).

## RESULTS AND DISCUSSION

**Synthesis and Structural Characterization of Four-Coordinate Iron(II) Phosphoraminate Complexes.** A series of trialkyl, alkyl/aryl, and triaryl phosphoraminate complexes 1–8 was prepared by reaction of PhB(MesIm)<sub>3</sub>Fe≡N and the respective phosphine at room temperature (Scheme 1). The phosphoraminate ligands in complexes 1–4 vary in both their steric and electronic properties, whereas the triaryl phosphoraminate ligands in complexes 5–8 are isosteric. Thus, these complexes allow both the steric and electronic properties of the phosphoraminate ligands on the spin-crossover behavior to be systematically investigated.

Many of these complexes have been structurally characterized by single-crystal X-ray diffraction (Figure 3). Comparison of the metrical parameters with the previously reported spin-crossover complex PhB(MesIm)<sub>3</sub>Fe–N=PPh<sub>3</sub> 5<sup>7</sup> is instructive, revealing that the nature of phosphine group influences the spin state of the iron complex. This is well-illustrated by the structural data for PhB(MesIm)<sub>3</sub>Fe–N=P(*p*-CF<sub>3</sub>C<sub>6</sub>H<sub>4</sub>)<sub>3</sub> 6 and PhB(MesIm)<sub>3</sub>Fe–N=PMe<sub>2</sub>Ph 2, both of which were obtained at 173(2) K. It is notable that the Fe–N, N–P, and Fe–C bond lengths for these two complexes are different (Table 1). Specifically, the Fe–N and Fe–C bond lengths are at least ~0.1 Å longer in complex 6 than that in 2, although the N–P bond length is slightly shorter in 6. These structural differences are similar to those observed between the high- and low-spin states of 5, where

Table 1. Selected Metrical Data for Iron(II) Phosphoramimato Complexes

complex	1	2	3	4	5 <sup>a</sup>		6	
phosphine	PMePh <sub>2</sub>	PMe <sub>2</sub> Ph	PMe <sub>3</sub>	P <sup>n</sup> Pr <sub>3</sub>	PPh <sub>3</sub>		P( <i>p</i> -CF <sub>3</sub> C <sub>6</sub> H <sub>4</sub> ) <sub>3</sub>	
T (K)	100(2)	100(2)	173(2)	100(2)	30(2)	150(2)	150(2)	
Fe–N (Å)	1.771(3)	1.769(3)	1.770(2)	1.754(3)	1.767(5)	1.807(1)	1.862(1)	
N–P (Å)	1.543(3)	1.541(3)	1.547(3)	1.556(3)	1.572(5)	1.549(2)	1.519(1)	
Fe–C (Å)	1.879(3)– 1.883(2)	1.865(3)– 1.873(3)	1.877(2)– 1.883(2)	1.857(3)– 1.872(3)	1.884(5)– 1.891(6)	1.939(2)– 1.954(2)	2.079(2)– 2.089(2)	2.073(1)– 2.106(2)
Fe–N–P (deg)	172.1(2)	175.7(2)	174.5(2)	178.0(2)	177.6(3)	171.0(1)	160.0(2)	176.3(1)
C–Fe–C (deg)	86.4(1)– 87.4(1)	86.3(1)– 87.3(1)	86.37(9)– 86.64(9)	86.0(1)– 86.5(1)	86.4(2)– 87.3(2)	85.28(9)– 89.20(9)	86.24(9)– 91.11(9)	86.57(5)– 88.80(5)

<sup>a</sup>Data from ref 7.

the Fe–C bonds are  $\sim 0.1$  Å and the Fe–N bond is  $\sim 0.05$  Å shorter in the low-spin state, and the N–P bond is shorter in the high-spin state. These structural data therefore suggests that **6** is in the high-spin state and **2** is in the low-spin state at this temperature.

The structural data for **1–4** reveals that all of these complexes are in the low-spin state at 100(2) K. The metrical parameters for most of these complexes are similar, with the exception of PhB(MesIm)<sub>3</sub>Fe–N=PMe<sub>3</sub>, **3**, which contains the smallest phosphine moiety. This complex has the shortest Fe–N and Fe–C bond lengths (average is 1.867(3) Å) of the series. It is also notable that the Fe–N and Fe–C bond lengths of complexes **1–4** are all shorter than the corresponding bond lengths in low-spin **5**. This suggests that although complex **5** does undergo spin-crossover, steric interactions between the phosphoramimato and the tris(carbene)borate ligands prevent the molecule from achieving the optimal low-spin geometry.

Some metrical parameters do not appear to be dependent on the nature of the phosphine. Thus, although the P=N bond is longer for all of these complexes than that in high-spin **5**, this metric does not correlate with the steric or electronic properties of the phosphine. In addition, the C–Fe–C and Fe–N–P bond angles are similar for all complexes.<sup>20</sup>

**Spin-Crossover in PhB(MesIm)<sub>3</sub>Fe–N=PR<sub>3</sub> (PR<sub>3</sub> = PMePh<sub>2</sub>, PMe<sub>2</sub>Ph, PMe<sub>3</sub> and P<sup>n</sup>Pr<sub>3</sub>) Complexes 1–4.** The spin-crossover behavior of complexes **1–4** was investigated in fluid THF-*d*<sub>8</sub> solution by <sup>1</sup>H NMR spectroscopy. As exemplified by the <sup>1</sup>H NMR spectra of PhB(MesIm)<sub>3</sub>Fe–N=PMe<sub>2</sub>Ph **2** (Figure 4), the high-temperature (328 K) <sup>1</sup>H NMR spectrum is paramagnetically shifted, with 11 resonances observed over a greater than a 100 ppm chemical shift window. The number and relative integration of the resonances is consistent with a three-fold symmetric structure having free rotation about the Fe–N–P linkage. The appearance of this spectrum is similar to other high-spin (*S* = 2) complexes of this tris(carbene)borate ligand.<sup>7,13g,n,o,21</sup> This high-spin state assignment is corroborated by the magnetic moment at this temperature, as determined by the Evans' method,  $\mu_{\text{eff}} = 4.3(3)\mu_{\text{B}}$  ( $\chi T = 2.3 \text{ cm}^3 \text{ K/mol}$ ).

Cooling the sample causes the chemical shift window to converge as the resonances shift toward the 0–10 ppm range typically observed for diamagnetic complexes. Thus, for example, the resonance assigned to the *ortho*-methyl protons of the tris(carbene)borate mesityl group show a steady change in chemical shift from  $\delta = -31.5$  ppm at 298 K to  $\delta = -1.7$  ppm at 200 K. This behavior is contrary to the anticipated Curie behavior of a simple paramagnet, where an expansion of

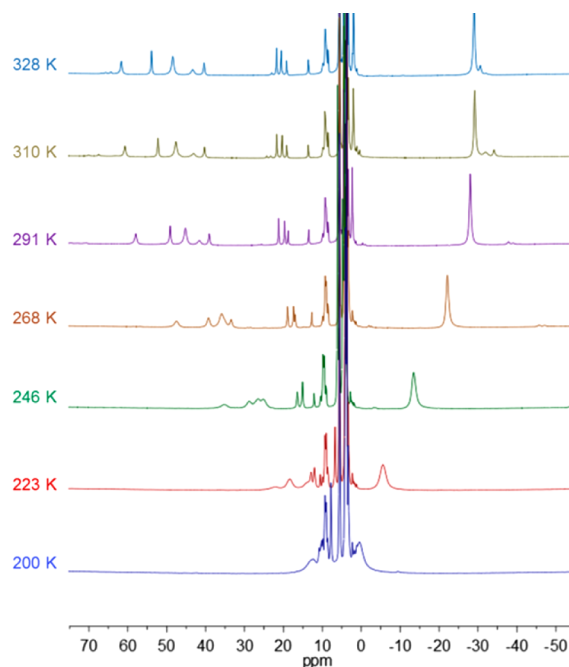


Figure 4. Temperature dependence of the NMR spectra for PhB(MesIm)<sub>3</sub>Fe–N=PMe<sub>2</sub>Ph **2** in THF-*d*<sub>8</sub> solution, showing the non-Curie behavior of the chemical shifts at low temperature.

the chemical shift window with decreasing temperature is expected. The magnetic moment of the complex at the lowest temperature probed, 200 K,  $\mu_{\text{eff}} = 1.7(3)\mu_{\text{B}}$  ( $\chi T = 0.36 \text{ cm}^3 \text{ K/mol}$ ), shows that the thermal behavior is associated with a high (*S* = 2) to low spin (*S* = 0) conversion, although a residual paramagnetic component results in the spin-crossover being incomplete at this temperature.

Plotting the chemical shift of each resonance as a function of temperature more clearly illustrates these changes (Figure 5). For each resonance, the change in chemical shift can be fit to the ideal solution model expression

$$\delta = \delta_{\text{LS}} + \frac{C}{T \left( 1 + \exp\left(\frac{\Delta H}{RT} - \frac{\Delta S}{R}\right) \right)} \quad (1)$$

where  $\delta_{\text{LS}}$  is the appropriate chemical shift in the low-spin state and *C* the relevant Curie constant. The assumptions of this equation, which have been previously described,<sup>22</sup> are (1) a Boltzmann distribution between the high- and low-spin states (i.e., spin-crossover); (2) Curie behavior for the chemical shift of the high-spin state; and (3) temperature independence for the chemical shift of the low-spin state.

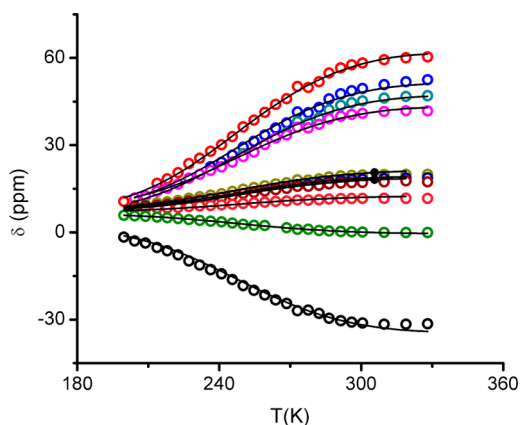


**Figure 5.** Plot of  $\delta$  versus  $T$  for selected resonances (Figure 4) of  $\text{PhB}(\text{MesIm})_3\text{Fe}-\text{N}=\text{PMe}_2\text{Ph}$  **2**. The solid lines are fits to the data for the ideal solution model. See the text for details.

Because complete conversion to the low-spin state is not observed, the chemical shifts in the low-spin state are not known. Where possible, these values are approximated using the chemical shifts of the diamagnetic complex  $\text{PhB}(\text{MesIm})_3\text{Fe}\equiv\text{N}$ .<sup>13j</sup> Small changes to these parameters are not found to significantly affect the fitting results. An excellent fit to the data is obtained, showing that this model adequately describes the spin equilibrium. The thermodynamic data obtained from this data fitting are provided in Table 2, with the spin-crossover temperature obtained from  $T_{1/2} = \Delta H/\Delta S$ .

Similar non-Curie behavior is observed for the chemical shifts of complexes **1**, **3**, and **4**, albeit with different temperature dependency (Figures S3–S8). As with complex **2**, the data for these complexes could also be fit to eq 1, giving the thermodynamic parameters enumerated in Table 2. Comparison of these thermodynamic data for complexes **1–4** shows that  $\Delta H$  and  $\Delta S$  are generally similar in magnitude to the corresponding values observed for six-coordinate iron(II) spin-crossover complexes.<sup>23</sup> Interestingly, there is little variation in the magnitude of  $\Delta S$ , whereas  $\Delta H$  increases with increasing  $T_{1/2}$ . This suggests that the differences in spin-crossover temperature can be attributed to differences in the relative strength of the iron-ligand bonds in each complex. It is notable that  $\Delta H$  for  $\text{PhB}(\text{MesIm})_3\text{Fe}-\text{N}=\text{PMe}_3$  **3** is markedly larger than the other complexes. This is likely a consequence of the shorter Fe–N and Fe–C bond lengths in **3** (at 100 K, see above), which will lead to greater orbital overlap and a larger ligand field splitting for the low-spin state.

Qualitatively,  $T_{1/2}$  for this series of complexes shows a similar trend to previous observations for six-coordinate complexes, i.e., increasing with increasing donor strength and decreasing size of the  $\text{PR}_3$  group. Assuming that the stereoelectronic properties of the phosphoraminate ligands are directly related to those of the corresponding phosphine moieties, more quantitative insight is obtained by correlating

the spin-crossover temperature against phosphine steric and electronic parameters, namely, the Tolman cone angle,  $\theta$ ,<sup>24</sup> and Bartik's  $\chi_T$ <sup>25</sup> value. Including complex **4** in these analyses is critical since the steric and electronic parameters of the  $\text{PMe}_x\text{Ph}_{3-x}$  series are correlated. The phosphine moiety in **4** ( $\text{P}^n\text{Pr}_3$ ) is larger than  $\text{PMe}_2\text{Ph}$ , but it is more strongly donating than  $\text{PMe}_3$ .

While there is a poor correlation between  $T_{1/2}$  and  $\chi_T$  (Figure S9), there is an excellent correlation with  $\theta$  (Figure 6). Thus, the spin-crossover temperature is primarily

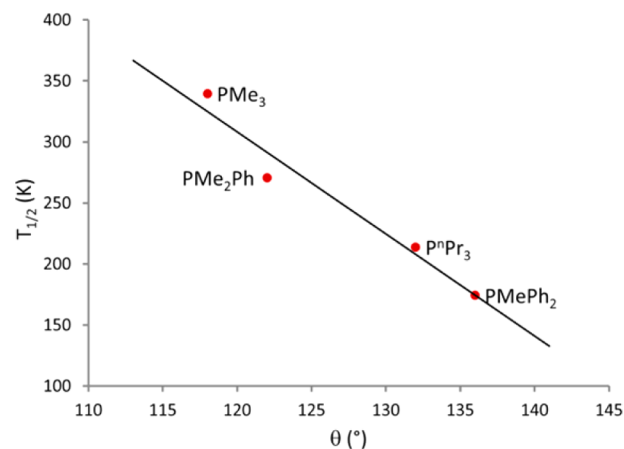


**Figure 6.** Plot of  $T_{1/2}$  versus Tolman cone angle ( $\theta$ ) for the respective phosphine. Equation of the best-fit line,  $T_{1/2} = -8.4(1.2)\theta + 1.3(2) \times 10^4$ .  $R^2 = 0.96$ .

influenced by the size of the phosphoraminate ligand, with smaller ligands favoring the low-spin state. The likely origin of this trend is the shorter metal–ligand bond lengths in the complexes containing the smaller phosphoraminate ligands, as suggested by the X-ray crystallographic data (*vide supra*). The shorter bond lengths increase the ligand field splitting and better stabilize the low-spin state.

**Spin-Crossover in  $\text{PhB}(\text{MesIm})_3\text{Fe}-\text{N}=\text{P}(p\text{-XC}_6\text{H}_4)_3$  ( $X = \text{H}, \text{CF}_3, \text{Me}$  and  $\text{OMe}$ ) Complexes **5–8**.** Because  $T_{1/2}$  for the complexes **1–4** is very strongly correlated with the size of the phosphine, the electronic effect of the phosphine group on the spin-crossover temperature cannot be determined. To address this issue, the spin-crossover behavior of the series of complexes **5–8** containing phosphoraminate ligands with *para*-substituted triarylphosphine groups has been investigated. Because these phosphines are the same size as measured by the Tolman cone angle, the spin-crossover behavior of the iron complexes is expected to be dependent only on the electronic properties of these ligands.

Because the spin conversion for these complexes occurs at temperatures that are too low to be investigated only by fluid solution measurements, the magnetic behavior of these complexes has been investigated by regular SQUID magnetometry (fluid and frozen solutions, respectively, above and

**Table 2. Summary of Results for Solution-Phase Spin-Crossover Behavior of Complexes **1–4****

complex	phosphine	$\theta$ (deg)	$\chi_T$ ( $\text{cm}^{-1}$ )	$\Delta H$ (kJ/mol)	$\Delta S$ (J/K/mol)	$T_{1/2}$ (K)
<b>1</b>	$\text{PMePh}_2$	136	2067.0	15.7(1.7)	87(9)	174(4)
<b>2</b>	$\text{PMe}_2\text{Ph}$	122	2065.3	19.5(0.4)	72(1)	271(1)
<b>3</b>	$\text{PMe}_3$	118	2064.1	28.2(1.2)	83(5)	340(2)
<b>4</b>	$\text{P}^n\text{Pr}_3$	132	2060.3	16.9(1.3)	79(6)	214(3)

below the melting temperature of the solvent). As exemplified by  $\text{PhB}(\text{MesIm})_3\text{Fe-N=PPh}_3$  **5**, thermally induced spin-crossover behavior is also manifested in these measurements (Figure 7). Interestingly, the spin-crossover temperature is

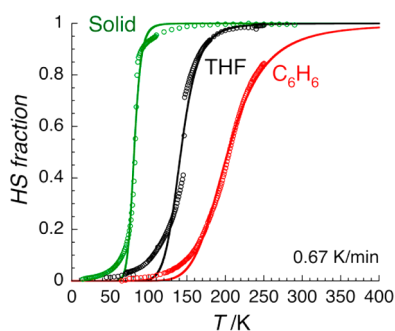


**Figure 7.** Temperature dependence of the high-spin fraction in  $\text{PhB}(\text{MesIm})_3\text{Fe-N=PPh}_3$  **5** in the solid state (1000 Oe) and solutions (at 1 T).

dependent on the medium, increasing from the solid state ( $T_{1/2} = 81$  K) to THF ( $T_{1/2} = 141$  K) to benzene ( $T_{1/2} = 203$  K). This solvent effect may reflect the change in the polarity of the complex that occurs on the spin-state change. Because the metal–ligand bonds are longer in the high-spin state, this increases the length of the molecule and consequently the dipole moment of the complex. The low-spin state, with its lower dipole moment, will be stabilized by lower polarity solvents, as is observed. Similar thermally induced spin-crossover is observed for complexes **7** and **8** (Figure S11 and S12) in the solid state ( $T_{1/2} = 118$  and  $64$  K, respectively) or in THF (Table 3); however, no evidence of a spin-state equilibrium was observed for **6** in the solid state, THF, or benzene (Figure S13)

**Table 3. Summary of Results for Spin-Crossover Behavior of  $\text{PhB}(\text{MesIm})_3\text{Fe-N=P}(p\text{-X-C}_6\text{H}_4)_3$  **5–8** in THF Solution**

complex	Ar-X	$3 \sigma_p$	$\Delta H$ (kJ/mol)	$\Delta S$ (J/K/mol)	$T_{1/2}$ (K)
<b>5</b>	H	0	14.9	106	141
<b>6</b>	$\text{CF}_3^a$	0.61			
<b>7</b>	Me	-0.51	11.7	75	156
<b>8</b>	OMe	-0.78	12.6	72	174

<sup>a</sup>Spin-crossover not observed.

In dilute solution, the data clearly show that  $T_{1/2}$  for this series of complexes increases with the donor strength of the *para*-substituent. For complexes **5**, **7**, and **8**, the electronic effect could be quantified by correlation with the Hammett parameter  $\sigma_p$  (Figure 8).<sup>26</sup> Interestingly, the slope of this Hammett plot is opposite to that observed for six-coordinate Fe(II) *Z*-2,6-di(1*H*-pyrazol-1-yl)-4-styrylpyridine complexes, where electron-withdrawing substituents on the ligand stabilize the low-spin state.<sup>27</sup> This difference is likely related to the nature of the frontier orbitals involved. In the case of the six-coordinate complexes, electron-withdrawing substituents are expected to increase the  $\pi$ -acceptor abilities of the ligand, lowering the energy of the  $t_{2g}$  orbital set, which stabilizes the low-spin state. For the four-coordinate complexes reported in this article, electron-donating substituents increase the phosphoraminate ligand  $\pi$ -donor

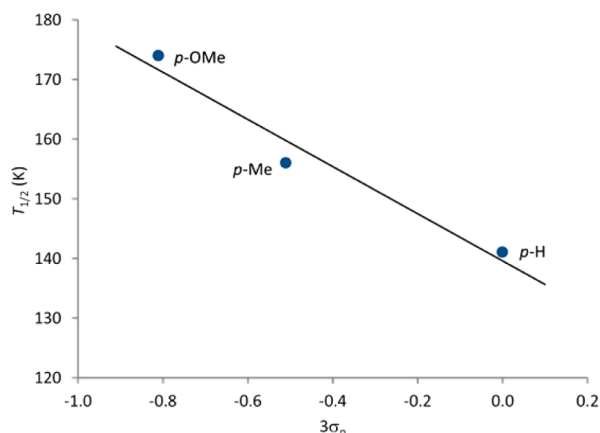


**Figure 8.** Plot of  $T_{1/2}$  versus  $3\sigma_p$  for complexes **5**, **7**, and **8**.

ability, increasing the energy of the  $e_{(b)}$  orbital set, which in turn stabilizes the low-spin state.

It should be noted, however, that despite the fact that there is an excellent correlation between  $T_{1/2}$  and  $\sigma_p$  for **5**, **7**, and **8** it is clear that this model does not appropriately describe the absence of spin-crossover behavior for **6**. Specifically, on the basis of the Hammett correlation, **6** is expected to undergo spin-crossover ( $T_{1/2} = 60$  K in frozen THF), which is not observed experimentally. The reasons for this discrepancy are not immediately apparent, but it is possible that the relationship between  $T_{1/2}$  and  $\sigma_p$  is not linear for positive  $\sigma_p$  values.

## CONCLUSIONS

In this work, we have obtained quantitative insight into the spin-crossover behavior of the four-coordinate iron(II) complexes,  $\text{PhB}(\text{MesIm})_3\text{Fe-N=PR}_3$ . In the case of mixed alkyl/aryl phosphoraminate ligands,  $T_{1/2}$  is linearly related to the size of the phosphine moiety, likely a consequence of steric interactions that hinder optimal metal–ligand orbital overlap with larger ligands. This quantitative relationship allows for unprecedented control over the spin state in iron(II) complexes that is further highlighted by the series of isosteric *para*-substituted triaryl phosphoraminate ligands, which demonstrate that more strongly donating phosphine groups stabilize the low-spin state. Given the unusual reactivity patterns of low-coordinate metal centers, these complexes offer the intriguing possibility of tunable spin-dependent reactivity.

## ASSOCIATED CONTENT

### Supporting Information

Further spectroscopic and magnetization data as well as additional crystallographic information. This material is available free of charge via the Internet at <http://pubs.acs.org>.

## AUTHOR INFORMATION

### Corresponding Authors

clerac@crpp-bordeaux.cnrs.fr  
smith962@indiana.edu

### Notes

The authors declare no competing financial interest.

## ■ ACKNOWLEDGMENTS

H.-J.L. and J.M.S. acknowledge funding from the NSF (CHE-1112299); J.J.S., D.S., and J.M.S. acknowledge funding from DOE-BES (DE-FG02-08ER15996). J.M.S. is a Dreyfus Teacher-Scholar. The Bruker X8 X-ray diffractometer was purchased via an NSF CRIF:MU award to the University of New Mexico (CHE-0443580). We thank Eileen Duesler for initial crystallographic measurements. R.C., D.S., and D.M. thank the University of Bordeaux, the ANR, the Région Aquitaine, and the CNRS for financial support.

## ■ REFERENCES

- (1) Halcrow, M. A. *Spin-Crossover Materials: Properties and Applications*; John Wiley and Sons, Ltd: Chichester, United Kingdom, 2013.
- (2) Gütlich, P.; Godwin, H. A. *Top. Curr. Chem.* **2004**, *233*, 1.
- (3) Claude, R.; Real, J.-A.; Zarembowitch, J.; Kahn, O.; Ouahab, L.; Grandjean, D.; Boukheddaden, K.; Varret, F.; Dworkin, A. *Inorg. Chem.* **1990**, *29*, 4442.
- (4) Müller, E. W.; Spiering, H.; Gütlich, P. *Chem. Phys. Lett.* **1982**, *93*, 567.
- (5) König, E.; Ritter, G.; Irlner, W.; Kanellakopoulos, B. *J. Phys. C: Solid State Phys.* **1977**, *10*, 603.
- (6) König, E.; Ritter, G.; Madeja, K.; Rosenkranz, A. *J. Inorg. Nucl. Chem.* **1972**, *34*, 2877.
- (7) Scepianiak, J. J.; Harris, T. D.; Vogel, C. S.; Sutter, J.; Meyer, K.; Smith, J. M. *J. Am. Chem. Soc.* **2011**, *133*, 3824.
- (8) Note that symmetry-allowed mixing of the  $e_{(a)}$  and  $e_{(b)}$  orbitals may complicate this simple picture; see McGarvey, B. R.; Telsler, J. *Inorg. Chem.* **2012**, *51*, 6000.
- (9) (a) Kennedy, B. J.; Fallon, G. D.; Gatehouse, B. M. K. C.; Murray, K. S. *Inorg. Chem.* **1984**, *23*, 580. (b) Thuery, P.; Zarembowitch, J. *Inorg. Chem.* **1986**, *25*, 2001.
- (10) Bowman, A. C.; Milsmann, C.; Bill, E.; Turner, Z. R.; Lobkovsky, E.; DeBeer, S.; Wieghardt, K.; Chirik, P. J. *J. Am. Chem. Soc.* **2011**, *133*, 17353.
- (11) Mossin, S.; Tran, B. L.; Adhikari, D.; Pink, M.; Heinemann, F. W.; Sutter, J.; Szilagyi, R. K.; Meyer, K.; Mindiola, D. J. *J. Am. Chem. Soc.* **2012**, *134*, 13651.
- (12) Selected reviews: (a) Mehn, M. P.; Peters, J. C. *J. Inorg. Biochem.* **2006**, *100*, 634. (b) Smith, J. M.; Subedi, D. *Dalton Trans.* **2012**, *41*, 1423. (c) Hohenberger, J.; Ray, K.; Meyer, K. *Nat. Commun.* **2012**, *3*, 720.
- (13) (a) Verma, A. K.; Nazif, T. N.; Achim, C.; Lee, S. C. *J. Am. Chem. Soc.* **2000**, *122*, 11013. (b) Brown, S. D.; Peters, J. C. *J. Am. Chem. Soc.* **2003**, *126*, 4538. (c) Brown, S. D.; Betley, T. A.; Peters, J. C. *J. Am. Chem. Soc.* **2004**, *125*, 322. (d) Hendrich, M. P.; Gunderson, W.; Behan, R. K.; Green, M. T.; Mehn, M. P.; Betley, T. A.; Lu, C. C.; Peters, J. C. *Proc. Natl. Acad. Sci. U.S.A.* **2006**, *103*, 17107. (e) Thomas, C. M.; Mankad, N. P.; Peters, J. C. *J. Am. Chem. Soc.* **2006**, *128*, 4956. (f) Rohde, J.-U.; Betley, T. A.; Jackson, T. A.; Saouma, C. T.; Peters, J. C.; Que, L. *Inorg. Chem.* **2007**, *46*, 5720. (g) Nieto, I.; Ding, F.; Bontchev, R. P.; Wang, H.; Smith, J. M. *J. Am. Chem. Soc.* **2008**, *130*, 2716. (h) Vogel, C.; Heinemann, F. W.; Sutter, J.; Anthon, C.; Meyer, K. *Angew. Chem., Int. Ed.* **2008**, *47*, 2681. (i) Scepianiak, J. J.; Fulton, M. D.; Bontchev, R. P.; Duesler, E. N.; Kirk, M. L.; Smith, J. M. *J. Am. Chem. Soc.* **2008**, *130*, 10515. (j) Scepianiak, J. J.; Young, J. A.; Bontchev, R. P.; Smith, J. M. *Angew. Chem., Int. Ed.* **2009**, *48*, 3158. (k) Moret, M.-E.; Peters, J. C. *J. Am. Chem. Soc.* **2011**, *133*, 18118. (l) Moret, M.-E.; Peters, J. C. *Angew. Chem., Int. Ed.* **2011**, *50*, 2063. (m) Scepianiak, J. J.; Vogel, C. S.; Khusniyarov, M. M.; Heinemann, F. W.; Meyer, K.; Smith, J. M. *Science* **2011**, *331*, 1049. (n) Scepianiak, J. J.; Bontchev, R. P.; Johnson, D. L.; Smith, J. M. *Angew. Chem., Int. Ed.* **2011**, *50*, 6630. (o) Scepianiak, J. J.; Margarit, C. G.; Harvey, J. N.; Smith, J. M. *Inorg. Chem.* **2011**, *50*, 9508. (p) Kuppuswamy, S.; Powers, T. M.; Johnson, B. M. J.; Bezpalko, M. W.; Brozek, C. K.; Foxman, B. M.; Berben, L. A.; Thomas, C. M. *Inorg. Chem.* **2013**, *52*, 4802. (q) Suess, D. M.; Peters, J. C. *J. Am. Chem. Soc.* **2013**, *135*, 4938.
- (14) (a) Jenkins, D. M.; Betley, T. A.; Peters, J. C. *J. Am. Chem. Soc.* **2002**, *124*, 11238. (b) Thyagarajan, S.; Shay, D. T.; Incarvito, C. D.; Rheingold, A. L.; Theopold, K. H. *J. Am. Chem. Soc.* **2003**, *125*, 4440. (c) Hu, X.; Meyer, K. *J. Am. Chem. Soc.* **2004**, *126*, 16322. (d) Shay, D. T.; Yap, G. P. A.; Zakharov, L. N.; Rheingold, A. L.; Theopold, K. H. *Angew. Chem., Int. Ed.* **2005**, *44*, 1508; **2006**, *47*, 7870. (e) Mehn, M. P.; Brown, S. D.; Jenkins, D. M.; Peters, J. C.; Que, L. *Inorg. Chem.* **2006**, *45*, 7417. (f) Cowley, R. E.; Bontchev, R. P.; Sorrell, J.; Sarracino, O.; Feng, Y.; Wang, H.; Smith, J. M. *J. Am. Chem. Soc.* **2007**, *129*, 2424.
- (15) (a) Tangen, E.; Conradie, J.; Ghosh, A. *J. Chem. Theory Comput.* **2007**, *32*, 448. (b) Wasbotten, I. H.; Ghosh, A. *Inorg. Chem.* **2007**, *46*, 7890.
- (16) Létard, J.-F.; Guionneau, P.; Goux-Capes, L. *Top. Curr. Chem.* **2004**, *235*, 221.
- (17) Mathonière, C.; Lin, H.-J.; Siretanu, D.; Clérac, R.; Smith, J. M. *J. Am. Chem. Soc.* **2013**, *135*, 19083.
- (18) For related studies of spin crossover in four-coordinate Co(II) complexes (solid state only), see: (a) Jenkins, D. M.; Peters, J. C. *J. Am. Chem. Soc.* **2003**, *125*, 11162. (b) Jenkins, D. M.; Peters, J. C. *J. Am. Chem. Soc.* **2005**, *127*, 7148.
- (19) (a) Watt, G. W.; Baye, L. J.; Drummond, F. O., Jr. *J. Am. Chem. Soc.* **1966**, *88*, 1138. (b) Brintzinger, H. H.; Bercaw, J. E. *J. Am. Chem. Soc.* **1970**, *92*, 6182.
- (20) A caveat to these observations is that the metrical parameters may also be influenced by packing effects in the solid state.
- (21) Smith, J. M.; Sutter, J.; Mayberry, D. E.; Wang, H.; Meyer, K.; Bontchev, R. P. *J. Am. Chem. Soc.* **2012**, *134*, 6516.
- (22) (a) Kläui, W.; Eberspach, W.; Gütlich, P. *Inorg. Chem.* **1987**, *26*, 3977. (b) Atkins, P.; de Paula, J. *Physical Chemistry*, 8th ed; Oxford University Press: Oxford, United Kingdom, 2006; Chapter 5.
- (23) Gütlich, P.; Hauser, A.; Spierling, H. *Angew. Chem., Int. Ed. Engl.* **1994**, *33*, 2024.
- (24) (a) Tolman, C. A. *Chem. Rev.* **1977**, *77*, 313. (b) Rahman, M. M.; Liu, H.-Y.; Eriks, K.; Prock, A.; Giering, W. P. *Organometallics* **1989**, *8*, 1.
- (25) Bartik, T.; Himmler, T.; Schulte, H.-G.; Seevogel, K. *J. Organomet. Chem.* **1984**, *272*, 29.
- (26) Hansch, C.; Leo, A.; Taft, R. W. *Chem. Rev.* **1991**, *91*, 165.
- (27) Takahashi, K.; Hasegawa, Y.; Sakamoto, R.; Nishikawa, M.; Kume, S.; Nishibori, E.; Nishihara, H. *Inorg. Chem.* **2012**, *51*, 5188.